METALS AND MATERIALS International, Vol. 12, No. 1 (2006), pp. 45~50

Effect of High Energy Ball Milling on Displacement Reaction and Sintering of Al-Mg/SiO_2 Composite Powders

K. D. Woo[1,*] and H. W. Huo[2,3]

[1] Division of Advanced Materials Engineering and the Research Center of Advanced Materials Development, Chonbuk National University, Deokjindong 1-ga, Deokjin-gu, Jeonju-si, Jeonbuk 561-756, Korea
[2] College of Life and Chemistry Science, Shenyang Normal University, Shenyang, 110034, P. R. China
[3] Post Doc. Fellow in the Research Center of Advanced Materials Development, Chonbuk National University, Korea

High-energy ball milling and low temperature sintering were successfully employed to fabricate a metal matrix composite of Al reinforced with Al_2O_3 particulate. Nano- and/or submicro-sized SiO_2 particles embedded in an Al-Mg matrix particle can be obtained by high-energy ball milling. No new phases were found in the high-energy ball milled Al-0.4 wt.%Mg-14 wt.%SiO_2 powder. Milling of the Al-Mg-SiO_2 powder increased the sintering rate and decreased the sintering temperature. The hardness of the sintered Al-Mg-SiO_2 composite using the ball-milled powder was about twice that of a sintered composite using a mixed powder due to the fine and homogeneous distribution of Al_2O_3 particles formed by the displacement reaction between Al and SiO_2 during sintering.

Keywords: high-energy ball milling, sintering, composite, displacement reaction

1. INTRODUCTION

Traditionally, aluminum matrix composites (AMCs) reinforced with particulates have been produced by such processing techniques as stir casting, powder metallurgy, squeeze casting, preform infiltration and spray forming [1-5]. During such processes, the reinforcing second-phase particulates (including borides, carbides, oxides, and nitrides) are combined with the matrix material (either in molten or powder form) by *ex situ* methods. Accordingly, the scale of the reinforcing phase is limited by the starting powder size, which is typically of the order of micrometers to tens of micrometers. In addition, the interfacial reaction and poor wettability between the reinforcements and the matrix due to surface contamination of the reinforcements are intractable [6,7]. Alternatively, *in situ* synthesis (i.e. displacement reaction) techniques can improve the above-mentioned shortcomings of *ex situ* methods by forming the particulates via a displacement reaction, which avoids contamination and yields satisfactory bonding strength and wettability with the matrix.

Furthermore, it is well known that the properties of metal matrix composites (MMCs) are controlled by the size and volume fraction of the reinforcements [6,8,9]. High mechanical properties and high wear resistance can be obtained when fine and thermodynamically stable ceramic particles are dispersed homogenously in the matrix [6-10]. In recent years, the mechanical alloying technique has been extensively used to fabricate MMCs reinforced with ceramic particulates formed by a displacement reaction. In combination with subsequent sintering, bulk composites reinforced with fine and thermodynamically stable ceramic particulates can be fabricated [11-13]. In this study, based on the chemical composition of A356 alloy, we selected a Al-0.4 wt.% Mg-14 wt.% SiO_2 powder mixture and investigated the effect of high-energy ball milling on the displacement reaction between Al and SiO_2 during sintering and mechanical property on sintering and hardness.

2. EXPERIMENTAL PROCEDURE

The materials used in the experiments were 99.5 % pure Al powder (average particle size 70 μm), Mg powder (average particle size 300 μm), and SiO_2 powder (average particle size 40 μm). The nominal composition of the powder mixture was Al-0.4 wt.%Mg-14 wt.%SiO_2. To produce

*Corresponding author: kdwoo@chonbuk.ac.kr

this powder, 7 g of a mixture of Al, Mg elemental powders, and SiO_2 powder was placed in a hardened steel vial together with 18 stainless steel balls 8.0 mm in diameter each. The ball to powder weight ratio was 4:1. The vial was then sealed in a glove box filled with high purity argon. The ball milling was performed using a SPEX8000 Mixer/Mill machine. After milling, the as-milled powders were analyzed using X-ray diffractometry (XRD) and differential thermal analysis (DTA) to identify the phase transformation during milling. The XRD analysis of the powders was performed in a Philips X-pert system diffractometer with Cu K_α radiation and a copper single crystal monochromator. A thermal analysis was performed to observe the effect of the milling time on the displacement reaction temperature of Al-0.4 wt.%Mg-14 wt.%SiO_2 powder by using a MTG 9600 DTA instrument under flowing argon. The heating rate used for the thermal analysis was 10 °C/min. The microstructure of the powder particles was examined using optical microscopy and JEOL JSM 5900 scanning electron microscopy. Both the as-mixed and the 8-h milled powders were uniaxially pressed at 30 MPa to form green compact discs 13 mm in diameter each. Then, the green compacts were sintered under different conditions in a tube furnace under flowing argon to fabricate the bulk sample based on the DTA analysis. The microstructure and elements distribution of the sintered products were examined with an SEM equipped with energy dispersive X-ray spectroscopy (EDX). Additionally, JEM-2010 transmission electron microscopy (TEM) was used to observe the particle size and distribution after milling.

3. RESULTS AND DISCUSSION

Figure 1 shows the XRD patterns of the powders milled at different times. For the as-mixed powder, the diffraction peaks corresponded to the Al and SiO_2 phases. The Mg phase could not be detected by XRD due to its trace quantity (Fig. 1(a)). After 1 h of milling, the XRD pattern (Fig. 1(b)) shows that the positions of the Al and SiO_2 peaks remained the same as those of pure Al and SiO_2 peaks, indicating that no significant reaction occurred during this initial period of milling; however, the intensity of the SiO_2 diffraction peaks decreased significantly. After 4 h of milling, the intensity of the Al peaks decreased, and the positions of the Al peaks remained unchanged, as shown in Fig. 1(c). This indicated that the amount of Mg diffusing into the Al phase is insignificant. After 4 and 8 h of milling, the Al peaks became obviously broadened. The widening of the XRD peaks was due to residual strain by the solid solution of Mg in the Al, as well as to a decrease of grain size.

Neglecting the contribution of the strain, the average grain size of the Al phase was estimated using the half height width of the Al {111} peak and Scherrer's equation [14]. The result showed that the average grain size of the Al phase decreased from 35 to 24 nm as the milling time was increased from 1 to 4 h. However, as the milling time was increased from 4 to 8 h, the average grain size changed slightly, from 24 to 20 nm.

Figures 2(a)-(d) shows the SEM micrographs of the powder particles in the powder mixture after 0, 1, 4, and 8 h of milling, respectively. For the as-mixed powder (0-h of milling), the original phases existed in separate powder particles. The aluminum particles appear as rods or spheres, and the brittle SiO_2 particles were angular. After 1 h of milling, the aluminum particles suffered deformation and fracture. The size of most of powder particles decreased significantly. Simultaneously, however, the soft Al particles in the initial starting mixture were affected by the cold working and the impact and shear forces generated by the milling media, and they tended to agglomerate to form larger powder particles; therefore, a few of the powder particles increased in size.

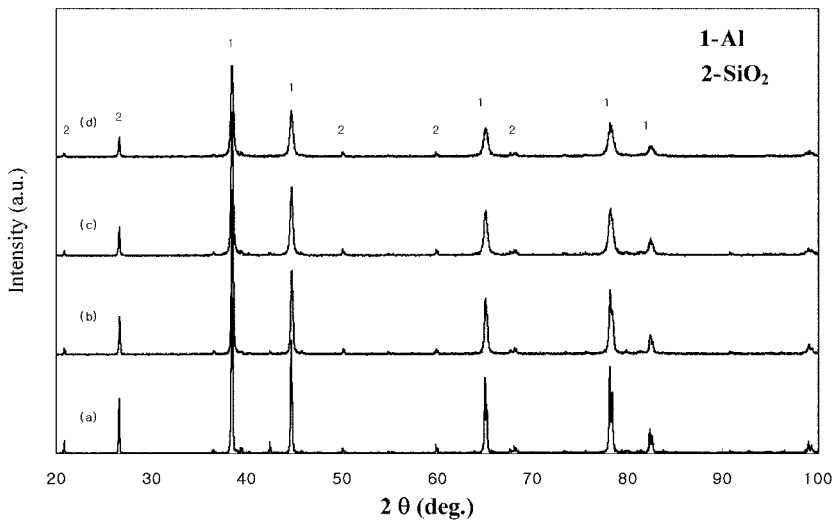

Fig. 1. XRD patterns of the milled powder for different times: (a) 0 h, (b) 1 h, (c) 4 h, and (d) 8 h.

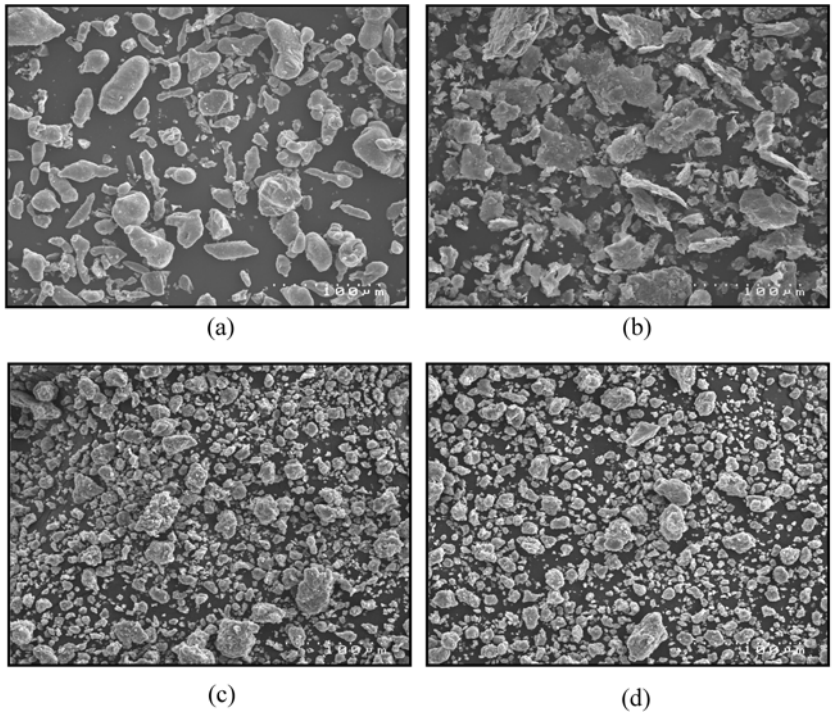

Fig. 2. SEM micrographs of the milled powders for different times: (a) 0 h, (b) 1 h, (c) 4 h, and (d) 8 h.

With further ball milling, the brittle SiO_2 particles were disintegrated continuously, and the size of the powder particles milled for 4 and 8 h exhibited a bi-modal distribution (Figs. 2(c) and (d)). The fine powder particles had sizes in the submicrometer or nanometer range, while the large powder particles had sizes in the range of 20-50 mm. Previous literature [15] has illustrated that diffusion couples will be generated during high-energy ball milling of the ductile-brittle system. A schematic diagram of the formation of diffusion couples is shown in Fig. 3 [15]. For the as-milled powder in this study, with the aid of SEM, it can be clearly seen that Al/SiO_2 diffusion couples were generated for the as-milled powders. The representative SEM micrographs of the 8-h milled powders are shown in Fig. 4. A great number of diffusion couples, consisting of SiO_2 particles embedded in a matrix of Al phase, were generated during ball milling.

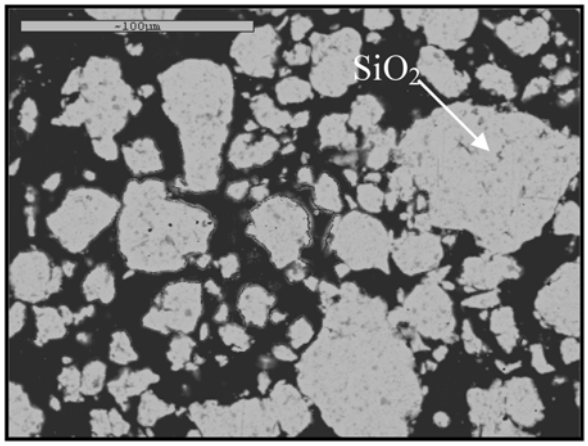

Fig. 4. SEM micrograph of the cross section of the 8-h milled powder particles.

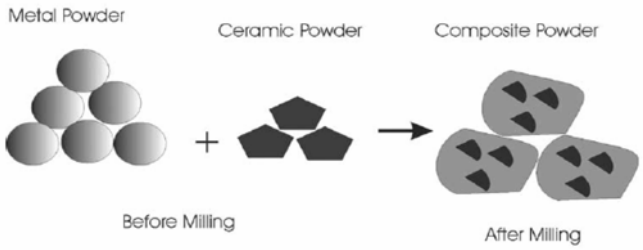

Fig. 3. Schematic diagram showing the formation of diffusion couples after high-energy ball milling [15].

Figure 5 shows (a) a bright field image (BFI) and (b) a corresponding selected area diffraction pattern (SADP) of the 4-h milled powders. It is clear that various amounts of brittle particles embedded in the Al alloy matrix for the 4-h milled powders. The SADP shows a ring-spot pattern that is characteristic of the simultaneous diffraction of crystal SiO_2 (fcc) and Al (fcc). This suggests that Al/SiO_2 diffusion couples formed during the ball milling. With the aid of image analysis software (Image Pro Plus), the sizes of particles embedded in the matrix were measured. After 4 h of milling, the

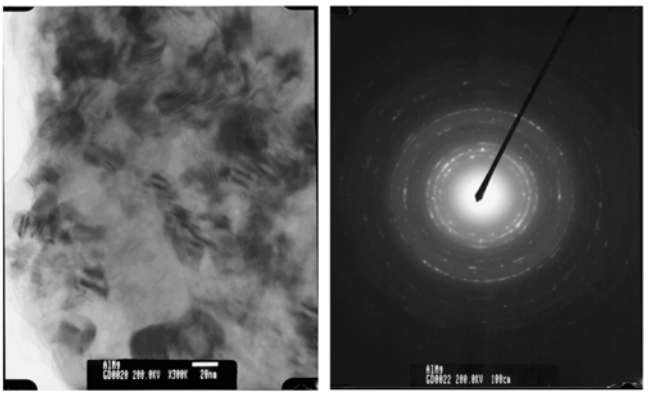

Fig. 5. TEM micrographs of the 4-h milled powder: (a) BFI and (b) SADP.

mean particle diameter of SiO_2 was about 53 nm. The mean particle diameter decreased with increased milling time. Thus, with an increase in milling time, the sizes of the diffusion couples decreased, and the volume fractions of the diffusion couples increased.

Figures 6(a)-(e) shows the DTA traces of the Al-Mg/SiO_2 powders milled for 0, 1, 4, 6, and 8 h, respectively. The DTA trace of the as-mixed powder showed only one endothermic peak due to the melting of aluminum. No other reactions took place during the process of heating the as-mixed powder. The DTA trace of the 1 h-milled powder exhibited one sharp endothermic peak followed by a small exothermic peak, which indicated that another reaction occurred besides the melting of aluminum. With a further increase of milling time for the 4 and 6 h milled powders, the DTA traces were similar to the trace of the 1 h milled powder. The main difference between the traces was that the exothermic peak became intensive with an increasing ball milling time. For the 8 h milled powder, the DTA trace exhibited one large exothermic peak in the temperature range of 530 ~ 680 °C, as well as one sharp endothermic peak superimposed on the exothermic peak. A comparison of the endothermic peak temperatures of the traces shows that the endothermic peak temperatures shifted to low temperatures with an increasing milling time. This can be interpreted as a dependence of the melting point on particle sizes and on the interface structure. Due to the particle size decrease and the embedding of SiO_2 particles into Al particles, the melting point of Al particles decreased with an increasing ball milling time. Á. Revesz *et al.* investigated the effect of milling time on the melting temperature of Al powder and reached similar conclusions as our study [16]. In addition, the exothermic peak became more intensive with an increasing milling time. This was the result of more SiO_2 particles embedded in the Al matrix. The longer the milling time, the more diffusion couples of Al/SiO_2 were formed. The more diffusion couples were formed, the more heat was released during the displacement reaction.

To identify the reaction corresponding to the exothermic peaks shown on the DTA traces, the as-milled powders were heated in a DTA instrument to different temperatures with argon protection, and then cooled to room temperature, before being subsequently analyzed using XRD.

Figure 7 shows the XRD pattern of the powders milled for 4 h heated to 680 °C. From this pattern, the SiO_2 peaks disappeared, while Al_2O_3 and Si peaks appeared, which suggested that the exothermic peak was caused by the displacement reaction between Al and SiO_2. The reaction is given by the following equation.

$$4Al(s, l)+3SiO_2(s)\rightarrow 2Al_2O_3(s)+3Si(s)+Q \quad (1)$$

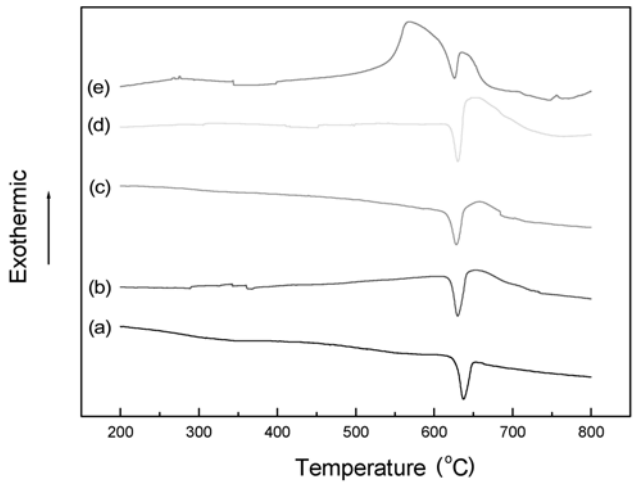

Fig. 6. DTA traces of the milled powders for different times: (a) 0 h, (b) 1 h, (c) 4 h, (d) 6 h, and (e) 8 h. The endothermic peak is caused by the melting of Al, and the exothermic peak is caused by the displacement reaction between Al and SiO_2.

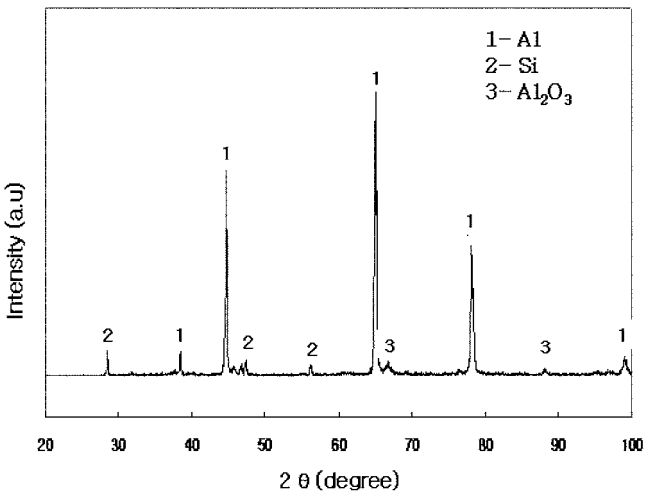

Fig. 7. XRD pattern of the 4-h milled powders heated to 680 using DTA equipment. Si and Al_2O_3 phases were formed by the displacement reaction during heating.

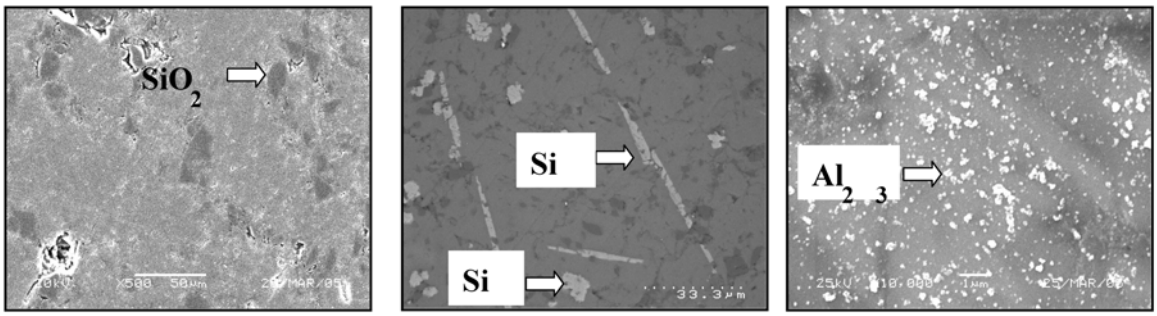

Fig. 8. SEM micrographs of sintered specimens: (a) the as-mixed powder sintered at 650 °C for 2 h, (b) 4-h milled powder sintered at 610 °C for 0.5 h and (c) 8-h milled powder sintered at 650 °C for 2 h.

In Eq. 1, the subscripts "s" and "l" stand for the solid and liquid forms of the substances. For the 1-, 4-, and 6-h milled powders, the exothermic peak followed the endothermic peak, and therefore, the exothermic reaction was liquid-solid reaction. However, for the 8-h milled powder, the exothermic reaction occurred in a large temperature range, and, at the initial stage, it was solid-solid reaction.

Based on the results of the DTA analysis, the preforms of the as-mixed and the as-milled powders were sintered under different conditions. Figure 8(a) shows the as-mixed powder preform sintered at 650 °C for 2 h, it was found that the as-mixed powder could be fully sintered, and the starting powder phases were integrated by metallurgy. However, particles of SiO_2 were still present and segregated on the grain boundaries, which would deteriorate the properties of the sintered production. No reaction occurred between SiO_2 and Al. Some voids were caused by the detachment of SiO_2 particles during polishing. For the 4-h milled powders, SEM micrograph of sintering at 610 °C for 0.5 h is shown in Fig. 8(b). It was found that Al_2O_3 particles and rod-shape Si particles were formed *in situ* by the displacement reaction between Al and SiO_2. For the 8-h milled powders, an SEM micrograph of sintering at 650 °C for 2 h is shown in Fig. 8(c). The SEM analysis also confirmed that the solid displacement reaction occurred during sintering and that fine Al_2O_3 particles, of less than 1 mm, were formed *in situ* and were dispersed homogeneously in the matrix. In accordance with Hanabe *et al.* [4], good wetting occurred between Al and SiO_2 because the change in the specific interfacial Gibbs free energy was a negative value. This negative value contributed to the spreading of liquid Al on SiO_2 particles particle. It is possible to infiltrate the metal into SiO_2 and form microcomposite Al_2O_3 reinforcements *in situ*. In addition, the displacement reaction was accompanied by an approximately 35 % volumetric contraction. After formation of a critical thickness of Al_2O_3 film on the SiO_2 particle, extensive cracking of this layer occurs. Such cracking permits the liquid Al to penetrate the SiO_2 further and to continue the reaction. [17]. By milling the SiO_2 and Al alloy powder, the size of SiO_2 particles of SiO_2 particle decreased to nano-size, and many cracks in the SiO_2 occurred. Therefore, it would be easy to penetrate a SiO_2 particle with Al atoms, even when using a lower sintering temperature.

Table 1 presents the hardness of different preforms sintered at 650 °C for 2 h. It can be seen that the hardness of the as-milled powders preform after the sintering treatment was twice that of the as-mixed powder preform. In addition, for the as-milled powders, the hardness of the sintered preform increased with an increasing milling time.

4. CONCLUSIONS

During the ball milling of Al-Mg/SiO_2 powder, soft Al particles underwent serious deformation and cold welding in the initial stage of milling, while the brittle SiO_2 particles were refined greatly with further milling. For 4- and 8-h milled powders, nano and/or submicro sized SiO_2 particle embedded in an Al-Mg composite particle resulted in the formation of diffusion couples. No new phases were formed during the high-energy ball milling. For the as-milled powder, an exothermic reaction consistent with the displacement reaction between Al and SiO_2 can be activated at a low temperature. The sintering rate was increased and the sintering temperature was decreased with an increase of the milling time of Al-Mg-SiO_2 powder. The hardness of the sintered compacts of the as milled powders was as about twice that of

Table 1. Hardness of different composites fabricated by sintering at 650 °C for 2 h

Specimen	as-mixed powder	1 h-milled powder	4 h-milled powder	8 h-milled powder
Hardness (HRB)	32.5	64.7	72.2	80.5

the sintered compact of the as-mixed powder due to the fine reinforcement particles and the homogeneous distribution of the Al_2O_3 particles formed by the displacement reaction.

ACKNOLEDGMENT

This work was supported by grant No R05-2004-000-10546-0 from Ministry of Science & Technology in Korea.

REFRENCES

1. J. Hashim, L. Looney, and M. S. J. Hashmi, *J. Mater. Process. Tech.* **92-93**, 1 (1999).
2. J. M. Torralba, C. E. da Costa, and F. Velasco, *J. Mater. Proc. Tech.* **133**, 203 (2003).
3. H. W Xing, X. M. Cao, W. P. Hu, L. Z. Zhao, and J. S. Zhang, *Mater. Lett.* **59**, 1563 (2005).
4. M. R. Hanabe and P. B. Aswath, *J. Mater. Res.* **11**, 1562 (1996).
5. S. K. Chaudhury, A. K. Singh, C. S. Sivaramakrishnan, and S. C. Panigrahi, *Mater. Sci. Eng. A* **393**, 196 (2005).
6. X. C. Tong and H. S. Fang, *Metall. Mater. Trans. A* **29**, 875 (1998).
7. S. C. Tjong and Z. Y. Ma, *Mater. Sci. Eng. R* **9**, 49 (2000).
8. B. S. S. Daniel, V. S. R. Murthy, and G. S. Murty, *J. Mater. Proc. Tech.* **68**, 132 (1997).
9. K. D. Woo, H. S. Na, S. W. Kim, T. Sato, and A. Kamio, *Met. Mater. -Int.* **7**, 613 (2001).
10. I. H. Song, D. K. Kim, Y. D. Hahn, and H. D. Kim, *Scr. Mater.* **48**, 413 (2003).
11. K. D. Woo and D. L. Zhang, *Curr. Appl. Phys.* **4**, 175 (2004).
12. D. Y. Ying and D. L. Zhang, *Mater. Sci. Eng. A* **286**, 152 (2000).
13. Y. Peng, C. J. Deng, N. G. Ma, and Dickon H. L. Ng, *Mater. Lett.* **58**, 679 (2004).
14. B. D. Cullity and S. R. Stock, *Element of X-Ray Diffraction, 3rd ed.*, p. 388, Prentice Hall, Inc. Upper Saddle River, New Jersey (2001).
15. D. L. Zhang, *Prog. Mater. Sci.* **49**, 537 (2004).
16. Á. RÉVÉSZ, *J. Mater. Sci.* **40**, 1643 (2005).
17. M. C. Breslin, J. Ringnalda, X. Xu, M. Fuller, J. Seeger, G. S. Daehn, T. Otani, and H. L. Fraser, *Mater. Sci. Eng. A* **195**, 113 (1995).